β_2-Adrenergic Receptor Signaling and Desensitization Elucidated by Quantitative Modeling of Real Time cAMP Dynamics*[S]

Jonathan D. Violin[‡1,2], **Lisa M. DiPilato**[§1,3], **Necmettin Yildirim**[¶1], **Timothy C. Elston**[‖4], **Jin Zhang**[**5], and **Robert J. Lefkowitz**[‡‡6]

*From the ‡Department of Medicine, Duke University Medical Center, §Department of Pharmacology and Molecular Sciences, The Johns Hopkins University School of Medicine, ¶Department of Mathematics, New College of Florida, ‖Department of Pharmacology, University of North Carolina, Chapel Hill, North Carolina 27599-7365, the **Department of Pharmacology and Molecular Sciences, The Solomon H. Snyder Department of Neurosciences and Department of Oncology, The Johns Hopkins University School of Medicine, and the ‡‡Departments of Medicine and Biochemistry, and Howard Hughes Medical Institute, Duke University Medical Center, Durham, North Carolina 27710*

G protein-coupled receptor signaling is dynamically regulated by multiple feedback mechanisms, which rapidly attenuate signals elicited by ligand stimulation, causing desensitization. The individual contributions of these mechanisms, however, are poorly understood. Here, we use an improved fluorescent biosensor for cAMP to measure second messenger dynamics stimulated by *endogenous* β_2-adrenergic receptor (β_2AR) in living cells. β_2AR stimulation with isoproterenol results in a transient pulse of cAMP, reaching a maximal concentration of ~10 μM and persisting for less than 5 min. We investigated the contributions of cAMP-dependent kinase, G protein-coupled receptor kinases, and β-arrestin to the regulation of β_2AR signal kinetics by using small molecule inhibitors, small interfering RNAs, and mouse embryonic fibroblasts. We found that the cAMP response is restricted in duration by two distinct mechanisms in HEK-293 cells: G protein-coupled receptor kinase (GRK6)-mediated receptor phosphorylation leading to β-arrestin mediated receptor inactivation and cAMP-dependent kinase-mediated induction of cAMP metabolism by phosphodiesterases. A mathematical model of β_2AR signal kinetics, fit to these data, revealed that direct receptor inactivation by cAMP-dependent kinase is insignificant but that GRK6/β-arrestin-mediated inactivation is rapid and profound, occurring with a half-time of 70 s. This quantitative system analysis represents an important advance toward quantifying mechanisms contributing to the physiological regulation of receptor signaling.

Tachyphylaxis, or desensitization, denoting the attenuation of a biological response to sustained or repeated intervention, is a pervasive phenomenon in physiological systems. For G protein-coupled receptors (GPCRs)[7] (or, more broadly, seven-transmembrane receptors), desensitization occurs through molecular mechanisms that can profoundly limit further stimulation of downstream signals, either through direct receptor inactivation or inhibition of downstream signaling. At the physiological level, we refer to this general loss of responsiveness as desensitization; we refer to the more specific case of direct inhibition of receptor molecules as "receptor inactivation." At the level of the receptor, GPCR signals represent a dynamic balance between ligand-stimulated activities, such as G protein coupling, and negative feedback mechanisms, such as receptor phosphorylation and β-arrestin recruitment (1). An agonist's efficacy is determined by the balance between these activities and is limited by the kinetics of receptor inactivation. Despite intensive research into the molecular mechanisms of desensitization by GPCR inactivation, the relative contributions of these mechanisms are largely unknown. One reason for this is that, until recently, there have been few techniques that directly measure receptor signaling in real time. Rather, data showing desensitization and receptor inactivation are usually based on either physiological assessments, such as hemodynamic parameters, which are too complex to derive mechanistic descriptions of receptor signal kinetics, or on molecular techniques with low temporal resolution. In particular, most mechanistic studies of

[S] The on-line version of this article (available at http://www.jbc.org) contains supplemental Figs. S1–S5 and Tables S1 and S2.
[1] These authors contributed equally to this work.
[2] Recipient of an American Heart Association postdoctoral fellowship.
[3] Recipient of National Institutes of Health F31 DK074381.
[4] To whom correspondence regarding mathematical modeling should be addressed: Dept. of Pharmacology, University of North Carolina, Chapel Hill, NC 27599-7365. Tel.: 919-962-8655; E-mail: telston@amath.unc.edu.
[5] Recipient of a Scientist Development Award from the American Heart Association, a Young Clinical Scientist Award from Flight Attendant Medical Research Institute, and a nontenured faculty award from 3M. To whom correspondence regarding ICUE2 should be addressed: 725 N. Wolfe St., Hunterian 307, Baltimore, MD 21205. E-mail: jzhang32@jhmi.edu.
[6] An investigator of the Howard Hughes Medical Institute. To whom correspondence should be addressed: Howard Hughes Medical Institute, Duke University Medical Center, Box 3821, Durham, NC 27710. Tel.: 919-684-2974; Fax: 919-684-8875; E-mail: lefko001@receptor-biol.duke.edu.

[7] The abbreviations used are: GPCR, G protein-coupled receptor; β_2AR, β_2-adrenergic receptor; CFP, cyan fluorescent protein; Epac, exchange protein directly activated by cAMP; FRET, fluorescence resonance energy transfer; GRK, G protein-coupled receptor kinase; IBMX, isobutylmethylxanthine; MEF, mouse embryonic fibroblast; PDE, phosphodiesterase; PKA, protein kinase A; RGS, regulator of G protein signaling; siRNA, small interfering RNA; YFP, yellow fluorescent protein.

cAMP Dynamics and β2-Adrenergic Receptor Regulation

the molecular regulation of receptor inactivation are performed with restimulation protocols, which compare signaling in naive cells to signaling in cells pretreated with a stimulatory pulse. In addition, in recent years, most such studies use overexpressed receptor (or broken cell preparations), which may alter physiological regulation by saturating signaling and feedback mechanisms.

The challenge of understanding signaling kinetics in living cells has begun to yield to newly developed techniques utilizing the growing families of fluorescent and luminescent biosensors, which can elucidate the spatial and temporal details of signal transduction (2). These sensors have been used to quantify ion concentration, protein translocation, protein turnover, protein-protein interactions, kinase activity, and protein conformational changes over time in living cells (2). Such data have substantially refined our understanding of molecular and cellular signaling and provide the opportunity to quantify the kinetic mechanisms underpinning receptor function.

The activation and desensitization of the archetypal β_2-adrenergic receptor (β_2AR) has been extensively studied, yet uncertainty remains regarding the relative contributions of the best characterized mechanisms of β_2AR inactivation: 1) cAMP-dependent kinase (PKA)-mediated phosphorylation and 2) G protein-coupled receptor kinase (GRK)-mediated phosphorylation followed by binding of the scaffold protein β-arrestin (1). We reasoned that quantitative molecular imaging with a live cell cAMP biosensor would allow us to test the effect of these mechanisms on β_2AR signaling kinetics. Furthermore, quantification of real time second messenger concentrations would allow us to develop, test, and refine a mathematical model of GPCR signaling and inactivation. Such a model would allow quantitative approximations and predictions of kinetic mechanisms of receptor regulation.

Thus, we set out to 1) develop an improved version of the cAMP reporter ICUE (indicator of cAMP using Epac) (3) with improved sensitivity and decreased ability to disrupt normal cell functions; 2) test the contribution of feedback mechanisms, including receptor inactivation on the kinetics of cAMP signals; and 3) develop a mathematical model for GPCR regulation with both descriptive and predictive capability.

EXPERIMENTAL PROCEDURES

ICUE2 Construction and in Vitro Characterization—ICUE2 was created by PCR using Epac1 as the template and amplifying from residue 149 to 881 incorporating KpnI and SacI restriction sites. The amplified Epac1 fragment was then fused to enhanced cyan fluorescent protein and citrine and cloned into pcDNA3 mammalian vector (Invitrogen) as previously described (3). *In vitro* dose-response experiments were performed using cell lysate from HEK-293 cells stably expressing ICUE2. Cells were lysed with nondenaturing mammalian lysis buffer, and fluorescence spectra were measured with a Fluoro-Max-3 fluorimeter (Jobin Yvon, Inc.) upon excitation at 434 nm before and after the addition of cAMP (Sigma). The EC$_{50}$ values were calculated using a sigmoidal dose-response equation (with variable slope),

$$\text{Ratio} = \text{Ratio}_{min} + \frac{\text{Ratio}_{max} - \text{Ratio}_{min}}{1 + 10^{\log(EC_{50} - X) \times \text{Hillslope}}} \quad \text{(Eq. 1)}$$

where X represents the logarithmic concentration, Ratio is the fluorescence resonance energy transfer (FRET) ratio response, and Ratio$_{min}$ and Ratio$_{max}$ are the minimum and maximum FRET ratios, respectively. FRET efficiency was determined by dissociation of citrine, the FRET acceptor, upon the addition of trypsin, as previously described (4).

ICUE2 in Cells—To measure intracellular cAMP concentrations, we determined the relationship of cAMP concentration to ICUE2 FRET loss by expressing ICUE2 in HEK-293 cells, collecting cellular lysate, blocking cAMP metabolism by the addition of 200 μM IBMX, and measuring the FRET ratio (cyan emission/yellow emission) in the presence of increasing concentrations of cAMP. This analysis revealed a simple sigmoidal dose-response relationship, analogous to ligand-receptor interaction, with an EC$_{50}$ = 12.5 $\pm$ 2.8 μM. This relationship allows us to calculate intracellular free cAMP from measured FRET ratios using the following equation,

$$[\text{cAMP}](\mu\text{M}) = \frac{12\mu\text{M} \cdot \text{Ratio}}{\text{Ratio}_{max} - \text{Ratio}} \quad \text{(Eq. 2)}$$

where Ratio represents the instantaneous FRET ratio, and Ratio$_{max}$ is the maximum change in FRET ratio determined by saturating ICUE2 with cAMP elicited from 50 μM forskolin in the presence of 200 μM IBMX. For analysis of whole cell cAMP responses, we averaged responses from a field of cells (10–30 cells) and averaged these responses across experimental replicates. Thus, all analysis herein ignores subcellular gradients of cAMP and instead reports the average concentration of cAMP experienced by diffusible proteins, such as ICUE2.

Cell Culture—HEK-293 cells were maintained in Dulbecco's modified Eagle's medium supplemented with 10% fetal bovine serum and 1% penicillin/streptomycin. Mouse embryonic fibroblasts (MEFs) were maintained similarly to HEK-293 except in high glucose Dulbecco's modified Eagle's medium. To establish ICUE2-stable HEK-293 cells, G418 at 500 μg/ml was used for selection and maintained at 250 μg/ml.

siRNA and Plasmid Transfection—HEK-293 cells were transiently transfected with FuGENE 6 transfection reagent (Roche Applied Science) or calcium phosphate and allowed to incubate for 12–24 h before imaging. MEF cells were transiently transfected with Lipofectamine 2000 reagent for 4–6 h and allowed to grow for 12–24 h in fresh medium before imaging. siRNA was transfected with GeneSilencer according to the manufacturer's instructions (Gene Therapy Systems).

Imaging—Cells were washed with Hanks' balanced salt solution buffer 24–72 h after transfection and imaged in the dark on a 37 °C temperature-controlled stage. Cells were imaged on a Zeiss Axiovert 200M microscope with MicroMAX BFT512 cooled charge-coupled device camera (Roper Scientific) controlled by METAFLUOR 6.2 (Universal Imaging) or SlideBook 4.0 (Intelligent Imaging Innovations). Dual emission ratio imaging used a 420DF20 excitation filter, a 450DRLP dichroic mirror, and 475DF40 and 535DF25 emission filters for CFP and YFP, respectively. The filters were alternated by a Lambda 10-2

filter changer (Sutter Instruments). Exposure time was 100–500 ms, and images were taken every 2–20 s. Background corrections of fluorescent images were carried out by subtracting the intensity of the background (autofluorescent cells and/or no cells) from the emission intensities of fluorescent cells expressing the reporters.

Immunoblotting—Cells were lysed in SDS sample buffer and adjusted to equal protein concentration by protein assay of a parallel set of cells. Equal amounts of protein were separated on 10% Tris-glycine polyacrylamide gels (Invitrogen) and transferred to polyvinylidine fluoride membranes for immunoblotting. GRKs were detected with isoform-specific antibodies from Santa Cruz Biotechnology, Inc. (Santa Cruz, CA) for GRK2 (sc-562), GRK3 (sc-563), GRK5 (sc-565), and GRK6 (sc-566), according to the manufacturer's instructions. Phosphorylated extracellular signal-regulated kinase 1/2, total extracellular signal-regulated kinase 1/2, and β-arrestin 2 were detected by immunoblotting with an anti-phospho-p44/42 MAPK antibody (1:3,000 dilution; Cell Signaling Technology, Beverly, MA), an anti-MAPK1/2 (1:10,000 dilution; Upstate Biotechnology, Inc., Lake Placid, NY), and a rabbit polyclonal anti-β-arrestin 2 antibody (A2CT) (1:5,000 dilution), respectively. Chemiluminescent detection was performed with horseradish peroxidase-coupled secondary antibody (Amersham Biosciences) and SuperSignal West Pico reagent (Pierce). Chemiluminescence was quantified by a charge-coupled device camera (Syngene ChemiGenius2); representative images are shown as *inverted grayscale*.

Supplemental Material—Fig. S1 shows the lack of effect of ICUE2 expression on β_2AR-mediated extracellular signal-regulated kinase signals. Fig. S2 shows that PKA inhibition has no effect on β-arrestin recruitment to the β_2AR. Fig. S3 shows that inhibition of $G\alpha_i$ signaling with pertussis toxin has no effect on cAMP dynamics. Fig. S4 shows the analysis of the mathematical model's parameter fitting. Fig. S5 shows the effect of simulating GRK overexpression on the mathematical model's simulation.

RESULTS

Development and Use of ICUE2 to Measure cAMP Dynamics—Recently, several laboratories have developed FRET-based indicators for cAMP. These biosensors are based on the guanine nucleotide exchange factor Epac (5), which is regulated by binding cAMP, resulting in conformational changes. Fusing Epac to the cyan and yellow variants of green fluorescent protein (CFP and YFP, respectively) allows detection of cAMP by measuring changes in intramolecular FRET attendant to cAMP-induced conformational changes (3, 6, 7). To probe receptor regulation most effectively, we engineered an improved version of ICUE1, our previously developed cAMP biosensor (3), to maximize signal detection and minimize perturbation of cellular functions. To accomplish this, we deleted the first amino-terminal 148 amino acids of Epac1, consisting of the DEP domain and an N′-terminal region responsible for membrane and mitochondrial targeting, respectively (8) (Fig. 1*A*). We named this biosensor ICUE2. Spectrophotometric measurement of the emission spectrum of ICUE2 in cell lysate demonstrated cAMP-dependent FRET changes; the addition of 1 mM cAMP decreases yellow emission (525 nm emission peak) and
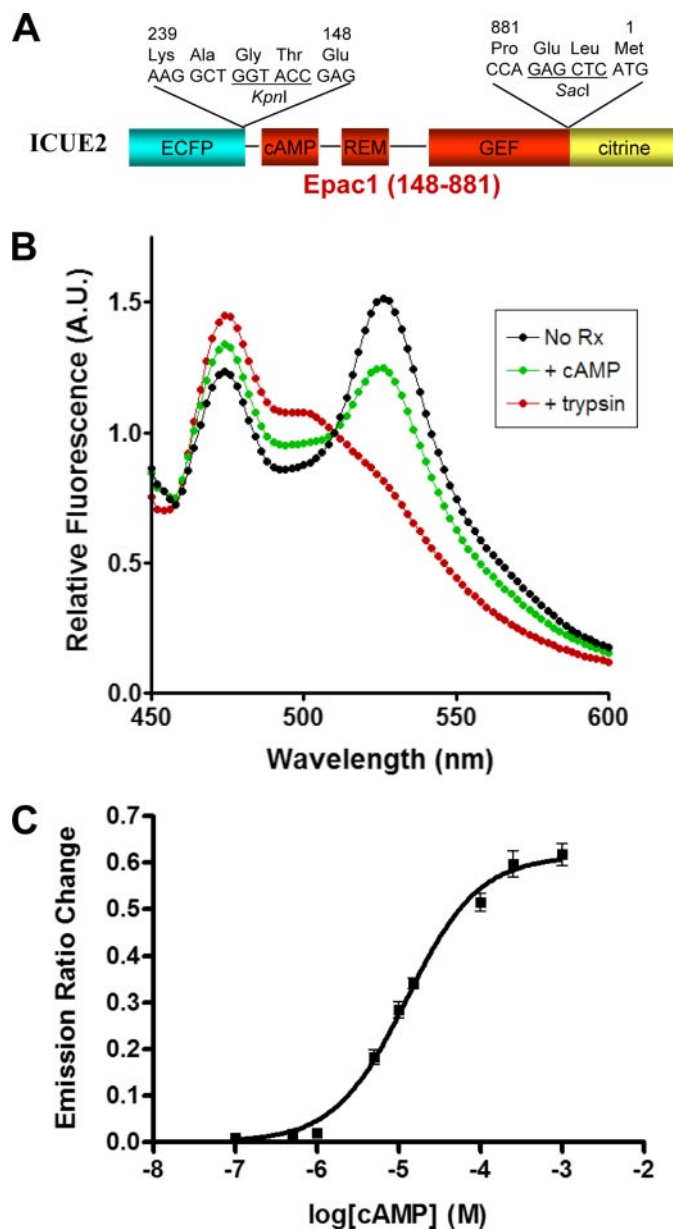
FIGURE 1. *In vitro* **characterization of ICUE2, an improved FRET-based cAMP reporter.** *A*, ICUE2 comprises EPAC1 (amino acids 148–881) fused between the cyan and yellow fluorescent proteins enhanced cyan fluorescent protein and citrine. *B*, spectra of purified ICUE2 without cAMP (*black*), with cAMP (*green*), and after trypsinization (*red*) show CFP emission (~485 nm) and YFP emission (~525 nm); the YFP peak is caused by FRET, since it is lost after trypsinization, and the amount of FRET depends on the presence of cAMP. *A.U.*, arbitrary units. *C*, ICUE2 from HEK-293 cell lysate incubated with varying concentrations of cAMP reveal a sigmoidal dose-response relationship of FRET change to cAMP concentration ($n = 3$), with an EC$_{50}$ of 12.5 ± 2.8 μM and Hill slope of 1.0.

increases cyan emission (485 nm emission peak), consistent with reduced FRET for cAMP-bound ICUE2 (Fig. 1*B*). We found a maximum change in FRET ratio (yellow emission intensity/cyan emission intensity) of 61%. The FRET signal was shown to be intramolecular by limited proteolysis, which cleaves CFP from YFP, and completely abrogates the yellow emission peak. By this technique, FRET efficiency values were calculated to be 30 and 11% before and after cAMP addition, respectively. We calibrated these FRET changes to cAMP con-
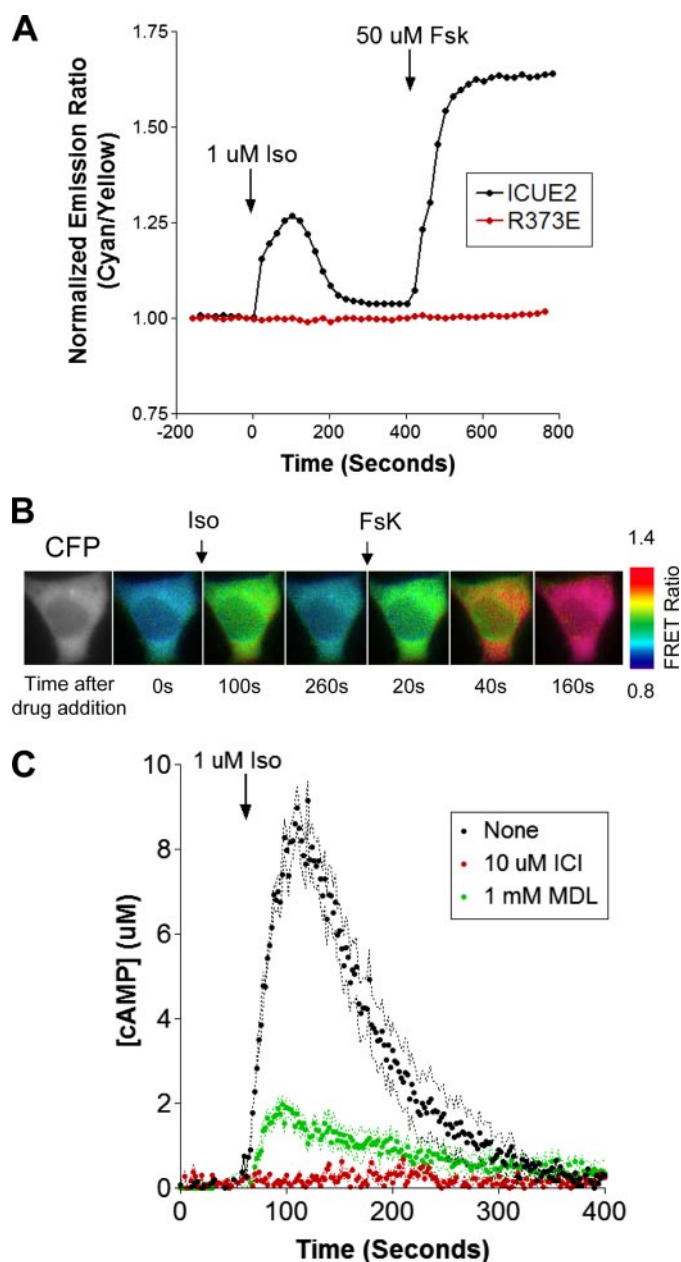
FIGURE 2. **Characterization of ICUE2 responses in HEK-293 cells.** *A*, a time course of ICUE2 FRET ratio (CFP emission/YFP emission) shows a transient decrease in FRET in response to 1 μM isoproterenol (*Iso*) (maximum FRET ratio change = 30 ± 2%, *n* = 15) and a larger, sustained FRET decrease in response to 50 μM forskolin (maximum FRET ratio change = 60 ± 2%, *n* = 15). In contrast, the cAMP-binding mutant ICUE2 R373E fails to respond to either stimulus. *B*, single cell FRET, displayed as *pseudocolor*, corresponding to the time course data shown in *A*. *C*, the isoproterenol-stimulated spike in cAMP is completely blocked by the β_2AR antagonist ICI-118,551 (10 μM) and mostly blocked by the adenylyl cyclase inhibitor MDL 12-330A (1 mM).

centrations (Fig. 1*C*), allowing us to measure cAMP responses quantitatively.

We then tested ICUE2 in living cells by transient transfection of HEK-293 cells, which express endogenous β_2AR at ~100 fmol/mg, or 90,000 receptors/cell (data not shown). We tested the ability of ICUE2 to respond to 1 μM isoproterenol and found a rapid and transient increase in FRET ratio (Fig. 2*A*). We then added 50 μM forskolin to maximally stimulate cAMP production, which increased the FRET ratio above that reached with

isoproterenol stimulation. This demonstrates that isoproterenol-induced cAMP is within the dynamic range of ICUE2. cAMP specificity was demonstrated with a variant of ICUE2 carrying the mutation R373E in the ICUE2 sequence, which destroys the cAMP binding pocket; this mutant did not respond to either isoproterenol or forskolin stimuli.

When expressed in cells, ICUE2 showed an even distribution of fluorescence throughout the cytoplasm, without the subcellular localization patterns observed with ICUE1 (3). This is consistent with the absence of membrane and mitochondrial targeting moieties caused by Epac1 truncation, as also seen with a different cAMP indicator (7). We visualized intracellular cAMP by pseudocolor representation of FRET ratio changes (Fig. 2*B*); this analysis revealed that ICUE2-detected changes in cAMP were uniform across the cell, as expected for an untargeted, diffusible reporter measuring a similarly diffusible analyte. Isoproterenol-stimulated cAMP reaches concentrations on the order of 10 μM (Fig. 2*C*). This response is sensitive to both the β_2AR antagonist ICI-118,551 and the adenylyl cyclase inhibitor MDL-12,330A. The transient cAMP response to isoproterenol is not unique to HEK-293 cells; we found a similar transient cAMP response to isoproterenol in rat vascular smooth muscle cells, indicating that cAMP dynamics are also rapid in more physiological cells (data not shown). In addition, ICUE2 does not alter downstream signaling, since ICUE2 expression does not significantly affect isoproterenol-stimulated extracellular signal-regulated kinase 1/2 activation, as might be expected from an Epac-based reporter (Fig. S1). Thus, we conclude that ICUE2 is a sensitive, relatively inert biosensor for intracellular cAMP.

Kinetics of β_2-Adrenergic Receptor-stimulated cAMP—Isoproterenol-stimulated cAMP responses display dose-dependent amplitude but surprisingly display largely dose-independent kinetics with similar times for peak cAMP concentration and duration for all concentrations of isoproterenol (Fig. 3*A*). Significant cAMP response was detectable at isoproterenol concentrations as low as 3 nM. These responses, converted to a single measurement by integrating cAMP concentration over time, display an EC$_{50}$ of ~20 nM (Fig. 3*B*), consistent with traditional measurements of isoproterenol-stimulated cAMP accumulation in HEK-293 cells. However, in contrast to traditional cAMP measurements, which usually rely on inhibition of phosphodiesterases (PDEs) to allow accumulation of significant cAMP concentration, ICUE2 measures cAMP in the native environment and thus reflects biological kinetics of cAMP responses. Indeed, the effect of PDE inhibition on cAMP responses is profound, demonstrating that PDE activity plays a critical role in limiting the magnitude and duration of cAMP signals (Fig. 3*C*). The residual cAMP clearance is probably caused by incomplete PDE inhibition and cAMP efflux from the cells.

We then set out to investigate the mechanisms that determine the duration of β_2AR stimulation of cAMP. Two classes of negative feedback regulation have been described for the β_2AR: "heterologous" mechanisms regulated by PKA and "homologous" mechanisms regulated by GRKs and β-arrestins (1). Inhibition of PKA with 20 μM H-89 resulted in profound enhancement of isoproterenol-stimulated cAMP (Fig. 4*A*). However, at
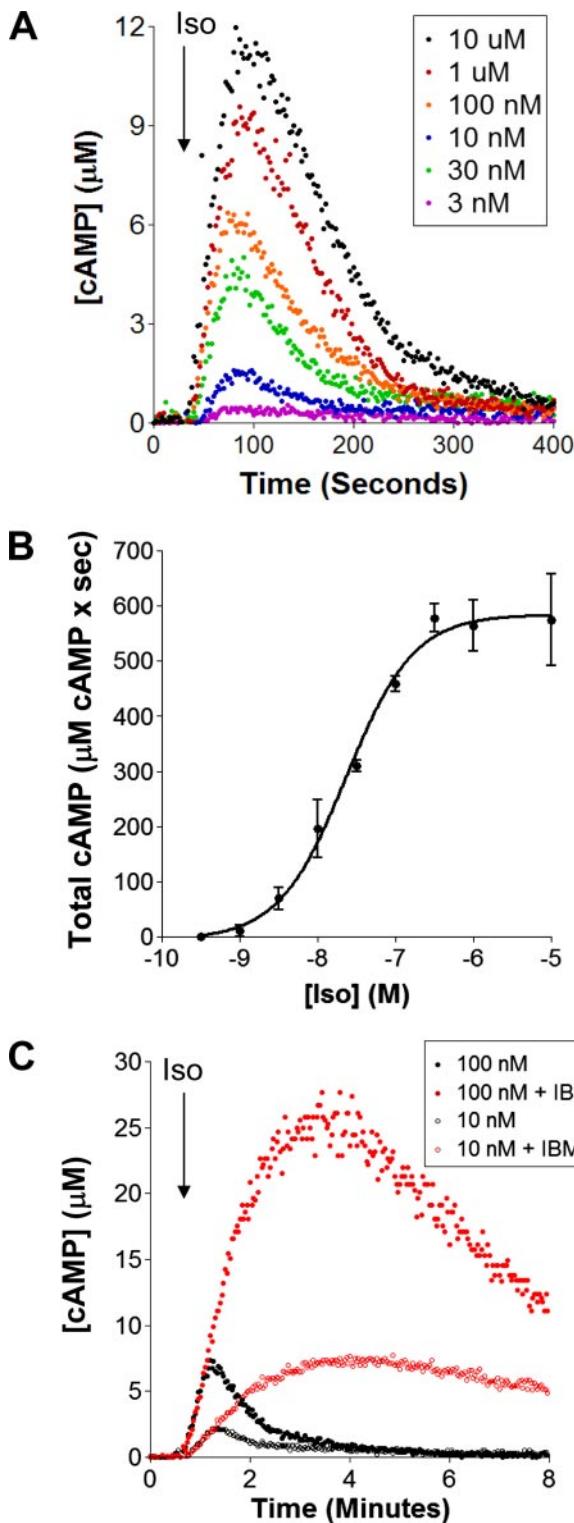
FIGURE 3. **β_2AR dose-response relationship for cAMP in HEK-293 cells.** *A*, increasing concentrations of isoproterenol (*Iso*) cause cAMP spikes of increasing magnitude but similar kinetics. *B*, the integrated ICUE2 response (area under curve) from *A* displays a sigmoidal dose-response relationship with EC$_{50}$ = 23 ± 1 nM and a Hill slope of 0.94 ± 0.2. *C*, inhibition of phosphodiesterase activity with 200 μM IBMX extends the cAMP response from 10 or 100 nM isoproterenol, demonstrating a PDE-limited clearance of cAMP.

least some of this effect is caused by regulation downstream of the receptor; H-89 also had a significant effect on forskolin-stimulated cAMP (Fig. 4*B*). This postreceptor regulation was
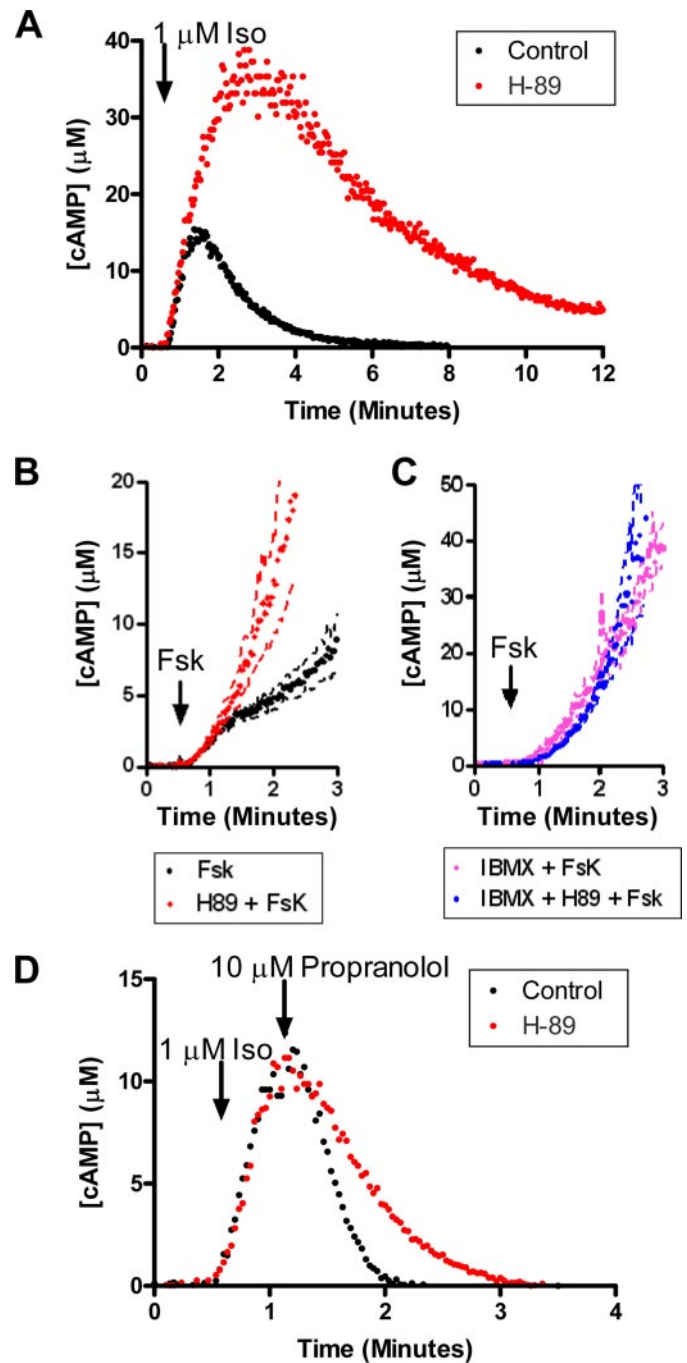

FIGURE 4. **PKA has multiple effects on β_2AR-mediated cAMP dynamics and β_2AR desensitization.** *A*, inhibition of PKA with 20 μM H-89 increases and extends the cAMP response to 1 μM isoproterenol. *B*, PKA inhibition with 20 μM H-89 increases cAMP generation from direct activation of adenylyl cyclase with 50 μM forskolin. *C*, pretreatment with 200 μM IBMX eliminates the effect of PKA inhibition on forskolin-stimulated adenylyl cyclase activity. *D*, PKA inhibition (20 μM H-89) slows the clearance of cAMP after isoproterenol stimulated receptor is inactivated with 10 μM propranolol.

caused by H-89-sensitive regulation of PDEs, since PDE inhibition eliminated the effect of H-89 on forskolin-stimulated cAMP (Fig. 4*C*). We also measured the effect of PKA on PDE activity for β_2AR signaling by blocking the receptor with 10 μM propranolol 30 s after isoproterenol stimulation, when cAMP concentrations are maximal; this allows measurement of the rate of cAMP clearance. H-89 resulted in a marked slowing of
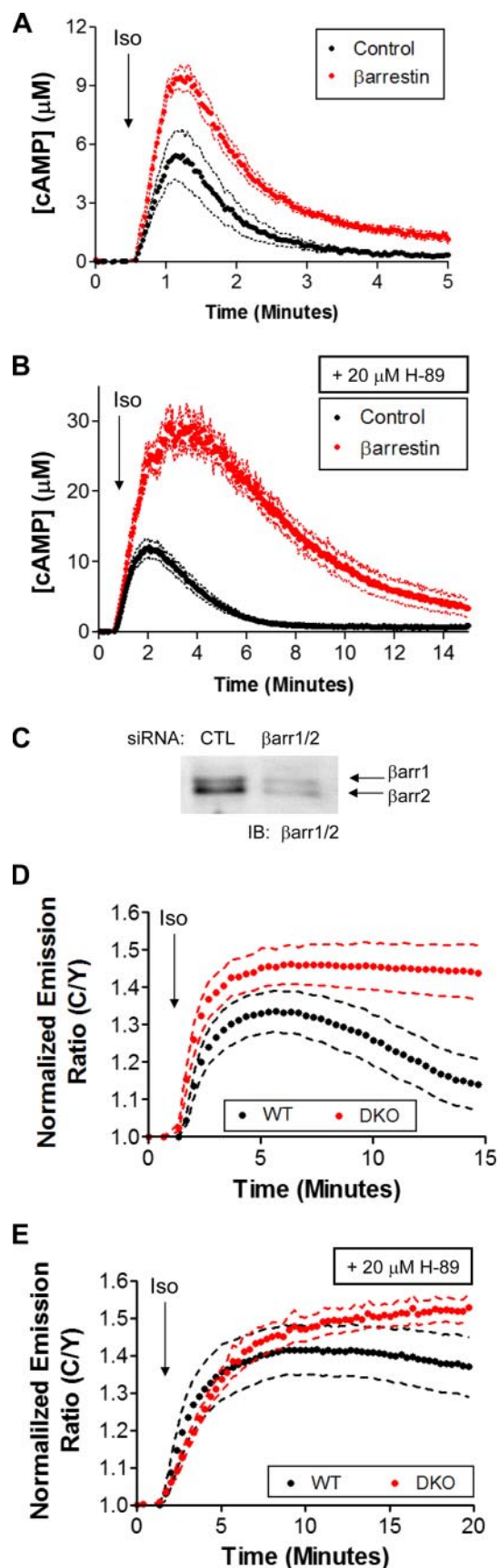
FIGURE 5. **siRNA-mediated silencing or genetic ablation of β-arrestin reduces β₂AR inactivation.** *A*, simultaneous silencing of β-arrestin 1 and β-arrestin 2 slightly increases cAMP stimulated by 1 μM isoproterenol (*Iso*).

cAMP clearance, consistent with a PKA-stimulated enhancement of PDE activity (Fig. 4*D*). Fidelity of this assay to cAMP clearance was verified by showing that the identical propranolol treatment of isoproterenol-stimulated cells results in rapid dissociation of β-arrestin from receptor ($t_{1/2} \sim 3$ s) (Fig. S2*A*); H-89 had no effect on this rate. The receptor is inactivated by propranolol treatment at least as rapidly as β-arrestin dissociation, indicating that the rate-limiting step in cAMP reduction after propranolol treatment is cAMP clearance. Since PKA has been shown to phosphorylate and activate PDE4 (9), the dominant PDE in our cells (data not shown), we conclude that PKA inhibits β₂AR-stimulated cAMP, at least in part, by PDE activation.

We then tested and ruled out other mechanisms of PKA regulation of β₂AR-mediated cAMP, including 1) phosphorylation and activation of GRK2 (10), 2) phosphorylation and switching of β₂AR from coupling to G_{α}s to G_{α}i (11), and 3) inhibition of adenylyl cyclase (12). We found that PKA does not significantly regulate GRK/β-arrestin function in our cells, since H-89 affected neither the amount nor the rate of isoproterenol-stimulated β-arrestin recruitment, a measure of GRK activity (13) (supplemental Fig. S2*B*). This result also demonstrates that despite the weak affinity of H-89 for the β₂AR (14), at the concentrations of H-89 and isoproterenol used here, H-89 does not directly interfere with β₂AR activation. In addition, under our experimental conditions, PKA did not promote coupling of the β₂AR to G_i-mediated inhibition of adenylyl cyclase (supplemental Fig. S3). We also found no evidence of PKA activation of adenylyl cyclase, since H-89 had no effect on forskolin-stimulated cAMP when PDEs were inhibited (Fig. 4*C*). Thus, the major postreceptor feedback mechanism in our cells is PKA activation of cAMP clearance by PDEs. However, the effects of this feedback and of direct receptor inactivation by heterologous (PKA-mediated) and homologous (β-arrestin/GRK-mediated) mechanisms are still unclear. We thus set out to quantify the contribution of each mechanism.

Homologous and Heterologous Mechanisms of β₂-Adrenergic Receptor Inactivation—To investigate β-arrestin function in β₂AR inactivation, we ablated β-arrestin 1 and β-arrestin 2 expression with siRNA-mediated silencing (15). In comparison with a nonsilencing control siRNA, an siRNA that targets both β-arrestins simultaneously increased and prolonged isoproterenol-stimulated cAMP concentrations (Fig. 5*A*). To rule out differences in β₂AR cell surface expression as a reason for altered cAMP responses, we measured cell surface receptor density by radioligand binding and found no significant changes after β-arrestin silencing (data not shown). The effect of β-arrestin siRNA on cAMP dynamics was dramatically

B, PKA inhibition (20 μM H-89) enhances the effect of β-arrestin 1/2 silencing on increased cAMP stimulated by 1 μM isoproterenol. *C*, β-arrestin 1/2 silencing averaged 75%, as shown by representative immunoblot. *D*, mouse embryonic fibroblasts transiently transfected with ICUE2 and stimulated with 1 μM isoproterenol display significantly increased and prolonged cAMP response in cells derived from β-arrestin 1/2 knock-out animals (*DKO*) when compared with cells derived from wild-type animals (*WT*), consistent with the nearly complete failure of β₂AR desensitization in the absence of β-arrestins. *E*, same experiment as in *A* but with pretreatment of 20 μM H-89 to inhibit PKA. Isoproterenol-stimulated cAMP is prolonged by PKA inhibition, but some desensitization is evident in wild-type MEFs. This desensitization is completely lost in β-arrestin 1/2 knock-out MEFs. *CTL*, control; *IB*, immunoblot.

amplified when cells were pretreated with H-89 to inhibit PKA-mediated desensitization mechanisms (Fig. 5*B*). However, some desensitization remained, despite blockade of all known mechanisms of negative feedback. This was explained by incomplete silencing of β-arrestin, which was at best 80% and averaged 75% (Fig. 5*C*), consistent with earlier findings (15, 16). Thus, the remaining desensitization was probably mediated by the unsilenced fraction of β-arrestins. To verify this, we tested isoproterenol-stimulated cAMP dynamics in MEFs from wild-type and β-arrestin 1/2 knock-out mice (17). We found that in MEFs transiently transfected with ICUE2 and stimulated with 1 μM isoproterenol, the absence of β-arrestins led to a pronounced loss of desensitization. This effect was amplified by H-89 inhibition of PKA, resulting in complete abrogation of desensitization (Fig. 5, *D* and *E*). This suggests that perfect β-arrestin silencing in HEK-293 cells would similarly result in complete disruption of β_2AR receptor inactivation when combined with PKA inhibition.

We also used siRNA to determine the role of GRKs in regulating cAMP dynamics. Since PKA stimulation of PDE may obscure the contributions of GRKs to β_2AR inactivation, we inhibited PKA activity with H-89 to isolate GRK- and β-arrestin-dependent desensitization. siRNA silencing of GRK2, GRK3, GRK5, or GRK6 revealed that only GRK6 has an effect on cAMP regulation in our HEK-293 cells; in the absence of GRK6, cAMP is amplified and prolonged (Fig. 6*A*). GRK silencing was confirmed by immunoblot (Fig. 6*B*), and radioligand binding studies showed no significant effect of GRK silencing on receptor expression (data not shown). We confirmed this result with a different siRNA sequence targeting GRK6, which similarly prolonged isoproterenol-stimulated cAMP, but also reduced β_2AR expression (data not shown). Thus, GRK6 is the most potent regulator of β_2AR inactivation among the GRKs expressed in HEK-293 cells. Overexpression of GRK6 had the opposite effect, dramatically speeding receptor inactivation (Fig. 6*C*); this indicates that GRK activity is the rate-limiting step in β_2AR inactivation and determines cAMP signal duration. Interestingly, overexpression of any other GRK also sped β_2AR inactivation, suggesting that GRK overexpression overcomes any GRK specificity arising from substrate sequence preference (data not shown).

These results are consistent with results showing GRK6 phosphorylation of the β_2AR to be the limiting step in receptor recruitment of β-arrestin and β-arrestin-mediated receptor inactivation in HEK-293 cells (13). However, the relative physiological contributions of the GRK and PKA desensitization mechanisms are still unclear, particularly since PKA can inhibit cAMP accumulation through both direct β_2AR inactivation and through stimulation of cAMP clearance by PDEs. Discrimination of these mechanisms is possible with the use of mutant receptors and PDEs, which are not regulated by PKA and/or GRK (9, 18). However, since even modest differences in receptor expression can alter signaling dynamics (16), we wanted to limit our analysis to signaling from endogenous wild-type receptors. We reasoned that the real time live cell cAMP concentration data generated by ICUE2 would be ideal for generating a quantitative mathematical model capable of specifying the contributions of PKA-mediated desensitization (including
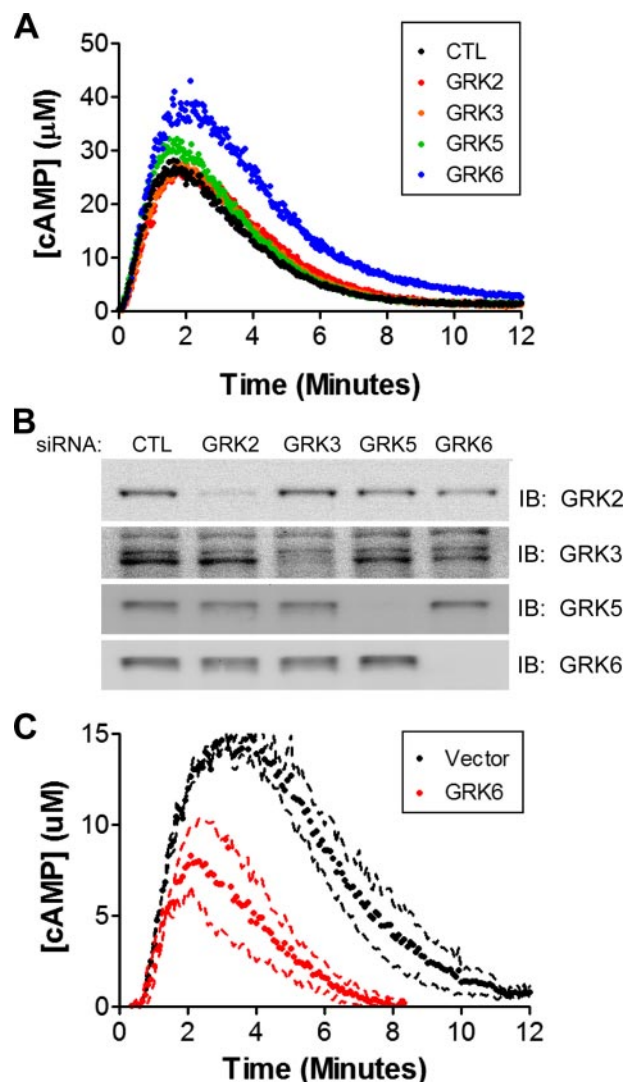

FIGURE 6. **siRNA-mediated silencing of GRKs reveals kinetic contributions of GRK6 to β_2AR inactivation.** *A*, GRK6 silencing, but not silencing of GRK2, GRK3, or GRK5, slows β_2AR inactivation after stimulation with 1 μM isoproterenol. PKA was inhibited with 20 μM H-89 to isolate the effects of GRK activity. *B*, GRK silencing by siRNA was more than 90% effective, as shown by a representative immunoblot for GRK2, GRK3, GRK5, and GRK6 in samples of equal protein concentration. *C*, overexpression of vector (pcDNA3.1) or GRK6 in HEK-293 cells, followed by inhibition of PKA (20 μM H-89) to isolate GRK/β-arrestin-dependent receptor inactivation, reveals that GRK6 can increase the rate of desensitization when overexpressed. *CTL*, control; *IB*, immunoblot.

receptor inactivation) and GRK/β-arrestin-mediated receptor inactivation.

A Quantitative Model of cAMP Dynamics—We thus synthesized a model of β_2AR cAMP signaling that captures each of the signaling events we have shown to affect cAMP dynamics as a series of ordinary differential equations. To maximize the predictive capability of our model, we limited its scope to only those relationships necessary to account for our data. Specifically, we describe the states of the receptor R as X-R-Z, where X denotes the state of the extracellular side of the receptor and Z denotes the state of the cytoplasmic side of the receptor. The extracellular states are ligated (L-) and empty (−). We modeled four cytoplasmic states: unphosphorylated (−), GRK-phosphorylated (-P$_{\text{GRK}}$), PKA-phosphorylated (-P$_{\text{PKA}}$), and β-arrestin-bound (-P$_{\text{GRK}}\beta$). This does not include receptors phosphoryla-

cAMP Dynamics and β₂-Adrenergic Receptor Regulation

ted by both PKA and GRK, which we assume to be functionally insignificant because of 1) the lack of effect of PKA inhibition on β-arrestin recruitment and 2) a low likelihood that PKA can phosphorylate GRK-phosphorylated, β-arrestin-bound receptor. We assume that the receptor and ligand are in equilibrium and that this equilibrium is not significantly affected by the cytoplasmic state of the receptor. In other words, if $[R]_{Total}$ is the total receptor concentration, then the following is true,

$$[R]_{Total} = ([L\text{-}R\text{-}] + [L\text{-}R\text{-}P_{GRK}] + [L\text{-}R\text{-}P_{PKA}] + [L\text{-}R\text{-}P_{GRK}\beta])$$

$$+ ([\text{-}R\text{-}] + [\text{-}R\text{-}P_{GRK}] + [\text{-}R\text{-}P_{PKA}] + [\text{-}R\text{-}P_{GRK}\beta]) = [L\text{-}R\text{-}Z]$$

$$+ [\text{-}R\text{-}Z] = [R]_{Total}\frac{[L]}{K_D + [L]} + [R]_{Total}\frac{K_D}{K_D + [L]} \quad \text{(Eq. 3)}$$

where K_D is the dissociation constant for the receptor-ligand complex, and $[L]$ is the concentration of the full agonist isoproterenol. We assume that receptor-ligand equilibrium is sufficiently rapid to be irrelevant to cAMP dynamics and thus that isoproterenol binding and displacement by propranolol are instantaneous. Thus, we follow only the time-dependent behavior of the concentrations of the various cytoplasmic states of the receptor. To constrain the model, we limited these states to either full activity or complete inactivity and ignored possible intermediate activity states. Thus, we assume that the ligated forms of the unphosphorylated and GRK-phosphorylated receptor are capable of signaling, since the GRK-phosphorylated receptor requires β-arrestin binding to fully desensitize (19, 20). The active receptor concentration $[R^*]$ is given by the following.

$$[R^*] = ([R\text{-}] + [R\text{-}P_{GRK}])\frac{[L]}{K_D + [L]} \quad \text{(Eq. 4)}$$

The other two states, $R\text{-}P_{PKA}$ and $R\text{-}P_{GRK}\beta$, represent inactive desensitized receptors.

We assume that GRK only phosphorylates the ligated receptor (21) and that this phosphorylation event is irreversible over the time span of the experiment, since the rate of β₂AR dephosphorylation after agonist withdrawal has been shown to be very slow (22). We assume that active PKA can phosphorylate both the ligated and ligand-free receptor and that this phosphorylation event is reversible, since dephosphorylation of PKA-phosphorylated β₂AR occurs much faster than GRK-phosphorylated β₂AR (22). These considerations lead to the following equation for the concentration of unphosphorylated receptor $[R\text{-}]$,

$$\frac{d[R\text{-}]}{dt} = -k_1[GRK]\frac{[L]}{K_D + [L]}[R\text{-}] - k_2[PKA^*][R\text{-}] + k_3[R\text{-}P_{PKA}]$$

(Eq. 5)

where $[PKA^*]$ is the concentration of active PKA, k_1 and k_2 are the rate constants for receptor phosphorylation by GRK and PKA, respectively, and k_3 is the rate constant for dephosphorylation of the PKA-phosphorylated receptor. The initial condition for this equation is $[R\text{-}] = [R]_{Total}$, since we assume that initially all the receptors are unphosphorylated. To simulate the

GRK silencing experiments, the GRK concentration is reduced by a factor α_2. Likewise, to simulate the PKA inhibition by H89, the total PKA concentration is reduced by a factor α_3.

We do not distinguish between β-arrestin 1 and β-arrestin 2, since both can bind to and desensitize GRK-phosphorylated β₂AR (17). Therefore, the concentration of GRK-phosphorylated receptor $[R\text{-}P_{GRK}]$ is given by the equation,

$$\frac{d[R\text{-}P_{GRK}]}{dt} = k_1[GRK]\frac{[L]}{K_D + [L]}[R\text{-}] - k_5[\beta][R\text{-}P_{GRK}] + k_4[R\text{-}P_{GRK}\beta]$$

(Eq. 6)

where $[\beta]$ represents the free β-arrestin concentration, k_4 is the rate constant for β-arrestin dissociation, and k_5 is the rate constant for β-arrestin binding. The initial condition for Equation 6 is $[R\text{-}P_{GRK}] = 0$. To simulate the β-arrestin silencing experiments, the total β-arrestin concentration is reduced by a factor α_1.

PKA-mediated G-protein switching and PKA inhibition of adenylyl cyclase do not contribute to cAMP dynamics in our cells (Figs. 4 and S3), so active adenylyl cyclase concentration $[AC^*]$ is given by the following,

$$\frac{d[AC^*]}{dt} = k_6\frac{[L]}{K_D + [L]}([R\text{-}] + [R\text{-}P_{GRK}])[AC] - k_7[AC^*] \quad \text{(Eq. 7)}$$

where k_6 represents the rate constant for adenylyl cyclase activation by the ligated receptor, and k_7 is the rate constant for basal deactivation of the enzyme. The initial condition is $[AC^*] = 0$. We assume that the intracellular ATP concentration remains constant and that PDE-mediated cAMP degradation follows Michaelis-Menten kinetics. We also assume that cAMP can be cleared by a PDE-independent mechanism,

$$\frac{d[cAMP]}{dt} = k_8[AC^*] - k_9[cAMP] - \frac{k_{10}[PDE^*][cAMP]}{K_M + [cAMP]} \quad \text{(Eq. 8)}$$

where k_8 is the pseudo-first order rate constant for cAMP production, k_9 is the rate constant for PDE-independent cAMP clearance, and k_{10} and K_m characterize PDE-mediated cAMP degradation. The initial condition is $[cAMP] = 0$. To simulate the experiments where PDE is inhibited by IBMX, the total PDE concentration is reduced by a factor α_4.

The equation for the concentration of active PKA, $[PKA^*]$, is as follows,

$$\frac{d[PKA^*]}{dt} = k_{11}[PKA][cAMP] - k_{12}[PKA^*] \quad \text{(Eq. 9)}$$

where k_{11} represents the rate constant for cAMP binding to PKA, and k_{12} is the rate constant for the dissociation of cAMP from PKA. Initially, $[PKA^*] = 0$. The equation for active PDE is as follows,

$$\frac{d[PDE^*]}{dt} = k_{13} + \frac{k_{14}[PKA^*]}{K_{M2} + [PDE]}[PDE] - k_{15}[PDE^*] \quad \text{(Eq. 10)}$$

where k_{13} is the rate constant for basal activation of PDE, k_{14} is the rate constant for PKA-dependent activation, and k_{15} is the rate constant for the deactivation of PDE. Because we have

included a basal activation rate for PDE, the initial concentration of active PDE is $[\text{PDE*}] = k_{13}/k_{15}$. Initially, all β-arrestin is in the free form and binds only to the GRK phosphorylated receptor.

$$\frac{d[\beta]}{dt} = k_4[\text{R-P}_{\text{GRK}}\beta] - k_5[\beta][\text{R-P}_{\text{GRK}}] \qquad \text{(Eq. 11)}$$

We do not consider protein turnover, since our experiments are less than 20 min long, so the total concentrations of receptor, adenylyl cyclase, PKA, PDE, and β-arrestin are constant and given by the following.

$$[\text{R}]_{\text{Total}} = [\text{R-}] + [\text{R-P}_{\text{GRK}}] + [\text{R-P}_{\text{PKA}}] + [\text{R-P}_{\text{GRK}}\beta] \quad \text{(Eq. 12)}$$

$$[\text{AC}]_{\text{Total}} = [\text{AC}] + [\text{AC*}] \qquad \text{(Eq. 13)}$$

$$[\text{PKA}]_{\text{Total}} = [\text{PKA}] + [\text{PKA*}] \qquad \text{(Eq. 14)}$$

$$[\text{PDE}]_{\text{Total}} = [\text{PDE}] + [\text{PDE*}] \qquad \text{(Eq. 15)}$$

$$[\beta]_{\text{Total}} = [\beta] + [\text{R-P}_{\text{GRK}}\beta] \qquad \text{(Eq. 16)}$$

These relations can be used to determine the concentrations of the remaining chemical species in the model. To fit the model equations to the experimental data (see supplemental material for details), all of the protein concentrations were scaled by their total amounts. In other words, we use the scaled variables $X' = [X]/[X]_{\text{Total}}$, where X denotes any of the protein species. Note that there is only one protein-protein complex in the model, R-P$_{\text{GRK}}\beta$. This requires that we specify the relative concentrations of receptor and β-arrestin. Based on radioligand binding experiments, which measured ~100 fmol/mg β_2AR in our HEK-293 cells (data not shown), and the fact that our HEK-293 cells only express sufficient β-arrestin 1/2 to desensitize 200 fmol/mg angiotensin II type 1 receptor (16), we took the effective concentration of β-arrestin to be twice that of the β_2AR. The full model consists of seven variables that satisfy Equations 3–11, five conservation relations given by Equations 12–16, and 22 free parameters. This information is summarized in supplemental Tables S1 and S2.

Model Validation, Parameter Estimation, and Simulations— To validate the model and perform parameter estimation, we used a Monte Carlo-based approach, using the Metropolis algorithm to fit the model to the experimental data (23, 24). A full description of the Monte Carlo optimization method can be found in the supplemental materials.

To ensure coherent data for this system level analysis, we repeated all of the modeled experiments in parallel, precluding day-to-day experimental variability as a source of error in our model. In fitting the model to the data, we did not place any constraints on the parameter values other than that they remain positive, with the exception of defining GRK6 silencing as reducing the effective activity of total GRK by 60%, consistent with our earlier results (13). We ran the Monte Carlo simulation until differences between the data and the model were minimized (supplemental methods and Fig. S4A) and evaluated each of the parameter estimations (Fig. S4B). The model captured all of the experimental manipulations remarkably well, as shown in Fig. 7. Some discrepancy between the model and the

experimental data were noted for GRK6 silencing, but we believe this to be an artifact in the data arising from the parallel experimental protocol that was used for the modeled data; when compared with data in a protocol optimized for GRK silencing (Fig. 6A), the model accurately predicts increases in both amplitude and duration of cAMP (See "Model Parameter Analysis" in the supplemental materials for an explanation of the relevant experimental differences for Figs. 6 and 7). The close fit of the data and the model suggests that despite the numerous assumptions made about β_2AR signaling mechanisms, the model captures the preponderance of mechanisms affecting cAMP dynamics in these cells. The model also accurately predicts data that were not fit, such as the effect of GRK overexpression; compared qualitatively with the experimental data (Fig. 6C), the model gives very similar results (Fig. S5).

We then used the model with our estimated parameters to simulate experiments selectively blocking phosphorylation of the β_2AR by either GRKs or PKA. Complete inhibition of GRK prevents β-arrestin recruitment to receptor (not shown), but 60% inhibition of GRK, as would be seen in siRNA silencing of GRK6, only slows the rate of β-arrestin recruitment (Fig. 8A). This is consistent with our previous results showing a slowed rate of isoproterenol-stimulated β_2AR recruitment of β-arrestin after GRK6 silencing (13). The model also predicts that complete ablation of GRK activity, which we have not been able to achieve experimentally, has a significant effect on β_2AR inactivation (Fig. 8B). In contrast, selectively blocking PKA phosphorylation of the β_2AR while preserving PKA phosphorylation of PDE, which we also cannot achieve with endogenous receptor, has no significant effect. Indeed, PKA-mediated receptor inactivation is predicted to be so weak that the model does not detect a difference between blockade of GRK-mediated inactivation alone and combined blockade of GRK- and PKA-mediated inactivation.

Thus, our model predicts that for endogenous β_2AR in HEK-293 cells, two mechanisms are responsible for limiting the duration of cAMP signals: receptor inactivation by GRK phosphorylation and β-arrestin recruitment and enhanced cAMP clearance by PKA activation of PDEs. Indeed, PKA activation of PDE accounts in full for the effect of global PKA inhibition. In the absence of this feedback mechanism, the remaining receptor inactivation is entirely through GRK phosphorylation and β-arrestin recruitment (Fig. 8C). Therefore, the only mechanism of direct receptor inactivation is β-arrestin recruitment, and the rate of β-arrestin recruitment is also the rate of receptor inactivation (Fig. 8D). In our model, active receptor has a half-life of 70 s, which is increased to 105 s by GRK6 silencing. This represents a surprisingly rapid inactivation of the β_2AR, which when combined with the PKA-mediated acceleration of PDE activity affords cells very strict regulation of cAMP dynamics.

DISCUSSION

Recently, there has been renewed interest in developing mathematical models of signaling pathways that are capable of predicting the temporal and spatial behavior of these systems (see Ref. 25 for a review). An important goal of these investigations is to establish the regulatory roles played by the multiple feedback and feed forward loops used to tightly control signal
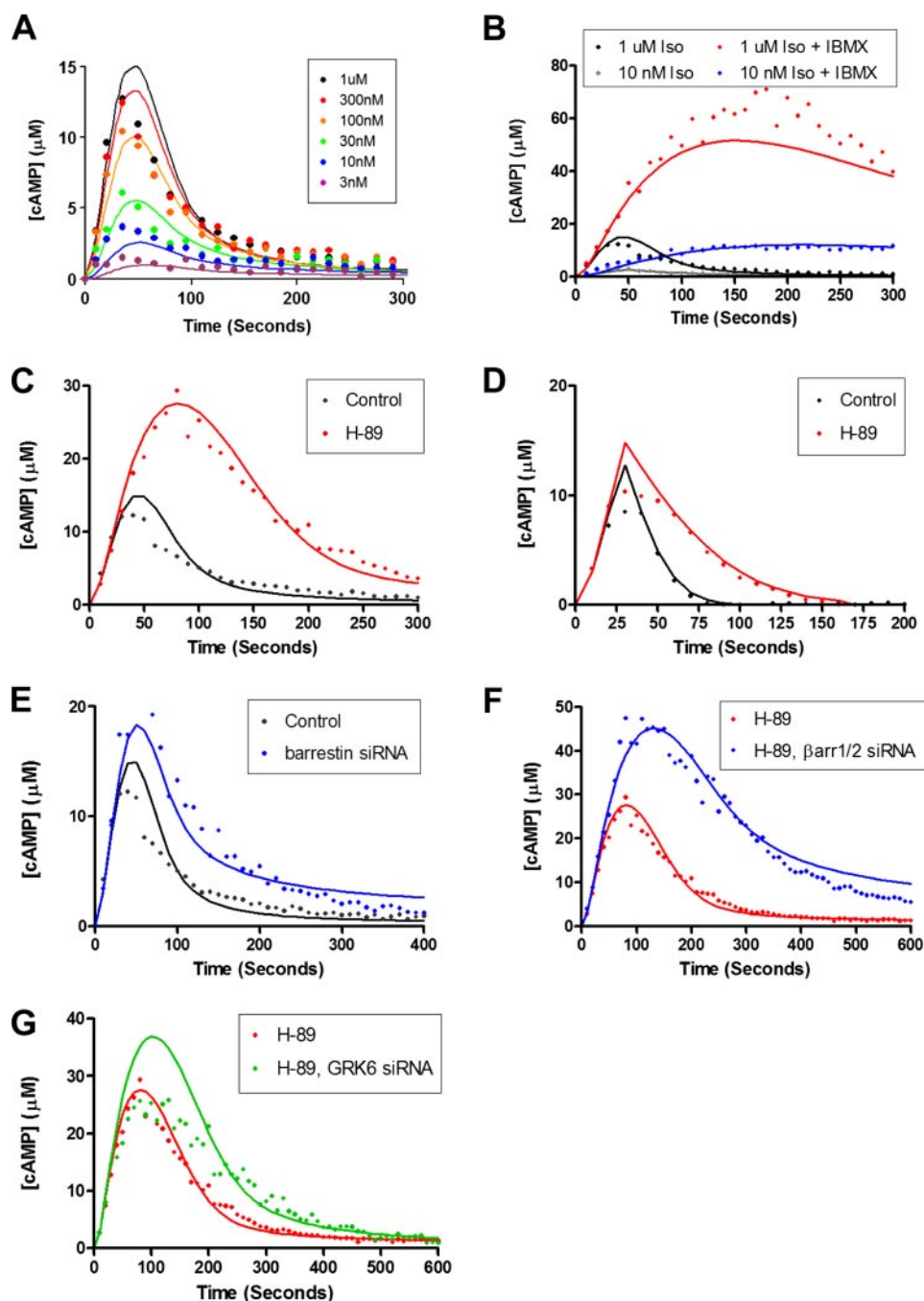
FIGURE 7. **Quantitative modeling of cAMP dynamics in HEK-293 cells.** Experimental data are displayed as points, and model simulations fit by Monte Carlo simulation are displayed as *lines*. *A*, cAMP responses across a range of isoproterenol concentrations. *B*, cAMP responses to 10 nM and 1 μM isoproterenol with and without IBMX inhibition of PDE activity. *C*, isoproterenol-stimulated cAMP response in cells transfected with a nonsilencing control siRNA, with or without H-89 inhibition of PKA. *D*, isoproterenol-stimulated cAMP response and clearance after propranolol inactivation of the β₂AR, with and without H-89 inhibition of PKA. *E*, isoproterenol-stimulated cAMP response after β-arrestin 1/2 silencing compared with a control siRNA. *F*, isoproterenol-stimulated cAMP response after β-arrestin 1/2 silencing compared with a control siRNA in the presence of H-89 inhibition of PKA. *G*, isoproterenol-stimulated cAMP response after GRK6 silencing compared with a control siRNA in the presence of H-89 inhibition of PKA.

such as the second messengers Ca^{2+}, inositol 1,4,5-trisphosphate, and cAMP (28–31), have exhibited higher temporal fidelity. However, the number of experiments used to validate the mathematical model is usually small, with model parameters often estimated "by eye" or by using nonlinear regression methods that produce a single optimal parameter set. Therefore, little consideration is given to how well the experimental data constrain the model parameters, if the optimal parameter set represents typical model behavior, or how sensitive model predictions are to the choice of parameter values. However, a more unbiased approach to developing quantitative models of signal transduction requires data with high fidelity to physiological signals, which is often not technically possible for intracellular signals.

ICUE2, a new FRET-based biosensor that measures absolute cAMP concentration sensitively and nondisruptively in living cells, reports cAMP dynamics with high temporal resolution and is thus ideal for developing and validating a mathematical model. Furthermore, monitoring GPCR signal transduction activity at the level of cAMP has several advantages. The transient activation of cAMP occurs on a rapid time scale, allowing us to ignore slow processes, such as transcriptional induction and protein degradation, and to discern more acute regulatory mechanisms, such as receptor inactivation and cAMP degradation. Furthermore, the relative proximity of the readout to receptor activity and the relatively small number of regulatory components simplified the development of our mathematical model.

ICUE2 allowed us to construct a model of receptor regulation that is capable of discriminating distinct mechanisms of receptor desensiti-

transduction. Many of these studies have focused on signaling by mitogen-activated protein kinase cascades; in general, these studies have relied on data sets consisting of sparse time courses for relative changes in protein levels or activity (*e.g.* phospho-mitogen-activated protein kinase measurements) (26, 27). A smaller number of models, based on more dynamic responses,

zation. Our model was developed and refined based on experimental results, using a combination of siRNA-mediated silencing and small-molecule inhibitors, as well as knock-out embryonic fibroblasts, which suggested that both GRK/β-arrestin-mediated homologous inactivation and PKA-mediated acceleration of cAMP clearance are important for regulating
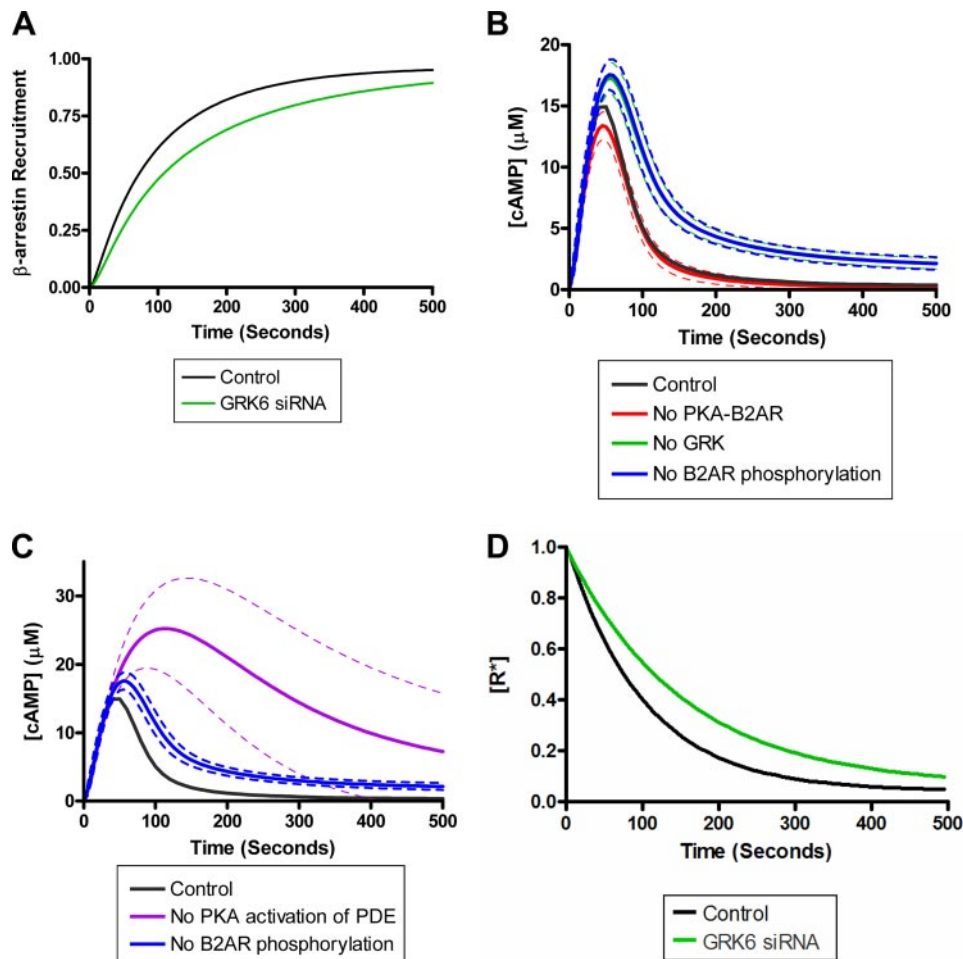
FIGURE 8. **Simulated results of theoretical experiments.** Monte Carlo simulation results are displayed as *solid lines*, with 95% prediction bands displayed as *dashed lines*. *A*, the rate of β-arrestin recruitment to the β₂AR is reduced by reducing GRK concentration by 60%. This reduction corresponds to the amount of GRK silencing found best to match the effect of GRK6 siRNA on cAMP dynamics and is similar to the effect of GRK6 silencing on measured β-arrestin recruitment (13). *B*, eliminating GRK phosphorylation of the β₂AR is predicted to have a significant effect on receptor inactivation. In contrast, eliminating PKA phosphorylation of the β₂AR while preserving PKA activation of PDE is not predicted to have any effect on β₂AR inactivation. Furthermore, blockade of all β₂AR phosphorylation is indistinguishable from blockade of GRK activity alone. *C*, selective blockade of PKA activation of PDE significantly prolongs predicted cAMP response but still allows for β₂AR inactivation. The combined effect of blocking PKA activation of PDE and blocking GRK phosphorylation of the β₂AR is predicted to be sustained cAMP, indicating complete loss of desensitizing activity. *D*, the rate of receptor inactivation, as calculated from the rate of β-arrestin recruitment. In the absence of significant PKA-mediated receptor inactivation, β-arrestin recruitment kinetics determine the rate of receptor inactivation. The half-life of active receptor is 70 s; this is slowed to 105 s by GRK6 siRNA.

β₂AR signals. However, we were unable to quantitatively determine the contribution of PKA-mediated heterologous inactivation for the endogenous receptor experimentally. Instead, we relied on our mathematical model to estimate the contribution of this mechanism. To maximize the robustness of such predictions, we developed our model to comprise the minimum number of parameters that would be constrained both by our data and the assumptions that we derived from the extensive literature on β₂AR regulation. No constraints were placed on the range of allowable parameter values other than that they all remain positive. The Monte Carlo method generated a family of parameter sets that all produced approximately equivalent fits to the data. The statistical distributions of these parameters serve as quantitative estimates of the true parameter values. This analysis revealed that in our system, cAMP-dependent activation of PDE by PKA was the dominant factor that con-

trolled signal amplitude and duration and that receptor inactivation is carried out exclusively by GRKs and β-arrestins.

Our model incorporates a number of assumptions that were required to reduce the model's degrees of freedom to a level that could be constrained by our experimental data. The most important of these assumptions are 1) ligand binding to receptor rapidly reaches equilibrium and is irrelevant to receptor signaling kinetics; 2) receptor signaling to adenylyl cyclase proceeds through one rate-limiting step and involves only two states of the receptor, "active" and "inactive"; 3) consistent with previous work, GRKs phosphorylate only active receptor and do so reversibly, whereas PKA phosphorylates either active or inactive receptor and does so irreversibly over the times we consider; and 4) consistent with the data described above, PKA reduces cAMP concentrations by two mechanisms: directly inactivating receptor and increasing PDE activity.

Most of the parameters were well constrained by the data, and all parameter sets produced similar predictions in regard to the relative roles of GRK- and PKA-mediated receptor inactivation and PKA-stimulated clearance in regulating cAMP dynamics. This is seen by the tight prediction bands shown in Fig. 8. The few parameters that were not well constrained displayed more complicated interrelationships (see supplemental materials for discus-

sion), but the fact that all of the parameter sets produced similar fits to the data and generated similar predictions provides compelling evidence for the validity of the model and accuracy of the predictions. Our results indicate that when tightly integrated with real time experimental analysis, mathematical modeling of signal kinetics provides a powerful tool for quantification of the biochemical processes that regulate signaling activity in living cells, even when these processes are not directly observable.

In contrast to recent studies that demonstrated compartmentalization of cAMP signaling (32), in our cells, and at the moderate spatial and temporal resolution we examined, we find that cAMP diffuses rapidly and uniformly throughout the cytoplasm. Therefore, it was not necessary to consider spatial gradients or localization effects. Further studies examining cAMP dynamics and GPCR regulation with greater spatiotemporal

resolution and in more physiological settings will afford the opportunity to expand our model to include spatial parameters (33). Indeed, such elaboration of mathematical models to encompass more complicated biology is a central aim of our systems biology approach. We hope that our model will serve as a relatively simple scaffold, sufficient to describe and predict GPCR regulation, upon which to cultivate more complicated models encompassing a wide range of pharmacological and physiological behaviors (31).

Because cAMP production occurs early in the β_2AR pathway, the number of mechanisms that regulate its activity is limited and reasonably well established. In fact, our model captured β_2AR signal kinetics with high fidelity by using only PKA-mediated and GRK/β-arrestin-mediated negative feedback. Thus, we did not model the effects of other regulatory mechanisms, such as regulator of G protein (RGS) protein activity (34). Importantly, our model does not discount significant RGS activity in regulating β_2AR signaling but rather did not detect *acute* changes in RGS activity that affected cAMP dynamics. In other cells that do display acute regulation by RGS activity or other mechanisms, our model will have to be expanded to incorporate such differences.

In particular, this study demonstrates that at physiological expression levels, the β_2AR is desensitized almost entirely by GRK/β-arrestin. Although this may not hold true in all tissues and cell types, our finding differs substantially from previous results, which found that PKA-mediated receptor phosphorylation is the major β_2AR-inactivating mechanism. However, these studies either did not evaluate the effect of PKA on cAMP clearance or used markedly overexpressed receptor (35–37). As our recent work has shown (16), even modest receptor overexpression can saturate the desensitizing capacity of β-arrestins, which operates via a stoichiometric mechanism. In contrast, PKA-mediated receptor inactivation operates enzymatically and thus is much less affected by receptor overexpression; thus, it is no surprise that in the context of artificially high receptor expression, desensitization mechanisms are artifactually biased away from GRK/β-arrestin. There is clear evidence that the β_2AR is phosphorylated by PKA and that this phosphorylation is amplified, relative to GRK-mediated phosphorylation, at low agonist concentrations (35). However, it is unclear how much these PKA-mediated phosphorylation events contribute to receptor inactivation. The results presented here suggest that β_2AR inactivation by PKA plays a minor role; even at low agonist concentrations, PKA inhibition is predicted to increase cAMP by blocking PDE activation but to have little effect on receptor activity (data not shown). Although the concentrations used here mimic receptor saturation by therapeutically used β-AR agonists, physiological β_2AR stimulation is mediated by lower concentrations of endogenous catecholamines (38). It will be important to test these predictions quantitatively both in more physiological systems, such as primary cell culture, and at lower agonist concentrations.

The experimental findings presented here illustrate the necessity of restricting quantitative analysis of signal transduction mechanisms to relatively undisturbed systems and highlight the opportunity presented by a systems biology approach. Our integrated development of a sensitive, nondisruptive bio-sensor and a quantitatively constrained mathematical model allowed us to test and characterize β_2AR signal transduction mechanisms with heretofore unseen precision. With continued advances in biosensor development, the systems biology approach undertaken here will lead to a much more quantitative understanding of signal transduction pathways and help elucidate the influence of specific molecular cues on physiological responses both in normal and pathological biology.

REFERENCES

1. Freedman, N. J., and Lefkowitz, R. J. (1996) *Recent Prog. Horm. Res.* **51,** 319–351
2. Zhang, J., Campbell, R. E., Ting, A. Y., and Tsien, R. Y. (2002) *Nat. Rev. Mol. Cell. Biol.* **3,** 906–918
3. DiPilato, L. M., Cheng, X., and Zhang, J. (2004) *Proc. Natl. Acad. Sci. U. S. A.* **101,** 16513–16518
4. Miyawaki, A., and Tsien, R. Y. (2000) *Methods Enzymol.* **327,** 472–500
5. de Rooij, J., Zwartkruis, F. J., Verheijen, M. H., Cool, R. H., Nijman, S. M., Wittinghofer, A., and Bos, J. L. (1998) *Nature* **396,** 474–477
6. Nikolaev, V. O., Bunemann, M., Hein, L., Hannawacker, A., and Lohse, M. J. (2004) *J. Biol. Chem.* **279,** 37215–37218
7. Ponsioen, B., Zhao, J., Riedl, J., Zwartkruis, F., van der Krogt, G., Zaccolo, M., Moolenaar, W. H., Bos, J. L., and Jalink, K. (2004) *EMBO Rep.* **5,** 1176–1180
8. Qiao, J., Mei, F. C., Popov, V. L., Vergara, L. A., and Cheng, X. (2002) *J. Biol. Chem.* **277,** 26581–26586
9. Sette, C., and Conti, M. (1996) *J. Biol. Chem.* **271,** 16526–16534
10. Cong, M., Perry, S. J., Lin, F. T., Fraser, I. D., Hu, L. A., Chen, W., Pitcher, J. A., Scott, J. D., and Lefkowitz, R. J. (2001) *J. Biol. Chem.* **276,** 15192–15199
11. Daaka, Y., Luttrell, L. M., and Lefkowitz, R. J. (1997) *Nature* **390,** 88–91
12. Houslay, M. D., and Milligan, G. (1997) *Trends Biochem. Sci.* **22,** 217–224
13. Violin, J. D., Ren, X. R., and Lefkowitz, R. J. (2006) *J. Biol. Chem.* **281,** 20577–20588
14. Penn, R. B., Parent, J. L., Pronin, A. N., Panettieri, R. A., Jr., and Benovic, J. L. (1999) *J. Pharmacol. Exp. Ther.* **288,** 428–437
15. Ahn, S., Nelson, C. D., Garrison, T. R., Miller, W. E., and Lefkowitz, R. J. (2003) *Proc. Natl. Acad. Sci. U. S. A.* **100,** 1740–1744
16. Violin, J. D., Dewire, S. M., Barnes, W. G., and Lefkowitz, R. J. (2006) *J. Biol. Chem.* **281,** 36411–36419
17. Kohout, T. A., Lin, F. S., Perry, S. J., Conner, D. A., and Lefkowitz, R. J. (2001) *Proc. Natl. Acad. Sci. U. S. A.* **98,** 1601–1606
18. Hausdorff, W. P., Bouvier, M., O'Dowd, B. F., Irons, G. P., Caron, M. G., and Lefkowitz, R. J. (1989) *J. Biol. Chem.* **264,** 12657–12665
19. Benovic, J. L., Kuhn, H., Weyand, I., Codina, J., Caron, M. G., and Lefkowitz, R. J. (1987) *Proc. Natl. Acad. Sci. U. S. A.* **84,** 8879–8882
20. Lohse, M. J., Benovic, J. L., Codina, J., Caron, M. G., and Lefkowitz, R. J. (1990) *Science* **248,** 1547–1550
21. Benovic, J. L., Strasser, R. H., Caron, M. G., and Lefkowitz, R. J. (1986) *Proc. Natl. Acad. Sci. U. S. A.* **83,** 2797–2801
22. Tran, T. M., Friedman, J., Baameur, F., Knoll, B. J., Moore, R. H., and Clark, R. B. (2007) *Mol. Pharmacol.* **71,** 47–60
23. Brown, K. S., Hill, C. C., Calero, G. A., Myers, C. R., Lee, K. H., Sethna, J. P., and Cerione, R. A. (2004) *Phys. Biol.* **1,** 184–195
24. Yu, Y., Dong, W., Altimus, C., Tang, X., Griffith, J., Morello, M., Dudek, L., Arnold, J., and Schuttler, H. B. (2007) *Proc. Natl. Acad. Sci. U. S. A.* **104,** 2809–2814
25. Kholodenko, B. N. (2006) *Nat. Rev. Mol. Cell. Biol.* **7,** 165–176
26. Bhalla, U. S., Ram, P. T., and Iyengar, R. (2002) *Science* **297,** 1018–1023
27. Sasagawa, S., Ozaki, Y., Fujita, K., and Kuroda, S. (2005) *Nat. Cell Biol.* **7,** 365–373
28. Lemon, G., Gibson, W. G., and Bennett, M. R. (2003) *J. Theor. Biol.* **223,** 93–111
29. Lemon, G., Gibson, W. G., and Bennett, M. R. (2003) *J. Theor. Biol.* **223,** 113–129

30. Xu, C., Watras, J., and Loew, L. M. (2003) *J. Cell Biol.* **161,** 779–791
31. Saucerman, J. J., Brunton, L. L., Michailova, A. P., and McCulloch, A. D. (2003) *J. Biol. Chem.* **278,** 47997–48003
32. Zaccolo, M., Magalhaes, P., and Pozzan, T. (2002) *Curr. Opin. Cell Biol.* **14,** 160–166
33. Saucerman, J. J., Zhang, J., Martin, J. C., Peng, L. X., Stenbit, A. E., Tsien, R. Y., and McCulloch, A. D. (2006) *Proc. Natl. Acad. Sci. U. S. A.* **103,** 12923–12928
34. Dohlman, H. G., and Thorner, J. (1997) *J. Biol. Chem.* **272,** 3871–3874
35. Tran, T. M., Friedman, J., Qunaibi, E., Baameur, F., Moore, R. H., and Clark, R. B. (2004) *Mol. Pharmacol.* **65,** 196–206
36. Seibold, A., Williams, B., Huang, Z. F., Friedman, J., Moore, R. H., Knoll, B. J., and Clark, R. B. (2000) *Mol. Pharmacol.* **58,** 1162–1173
37. Vaughan, D. J., Millman, E. E., Godines, V., Friedman, J., Tran, T. M., Dai, W., Knoll, B. J., Clark, R. B., and Moore, R. H. (2006) *J. Biol. Chem.* **281,** 7684–7692
38. de Champlain, J., Farley, L., Cousineau, D., and van Ameringen, M. R. (1976) *Circ. Res.* **38,** 109–114